Submitted to the
XXXII$^{\mathrm{nd}}$ International Conference on High Energy Physics
16-22 August 2004, Beijing, China

Abstract: 6-0249 **Parallel Session: QCDsoft**

Diffractive photoproduction of dijets at HERA

ZEUS Collaboration

Abstract

The diffractive photoproduction of dijets has been studied using $77.6\,\mathrm{pb}^{-1}$ of data taken by the ZEUS detector at HERA. The measurements have been made in the kinematic range $0.2 < y < 0.85$ and $x_{I\!P} < 0.035$, where y is the inelasticity and $x_{I\!P}$ is the fraction of the proton momentum taken by the diffractive exchange. The jets are reconstructed using the longitudinally invariant k_T algorithm and the two highest transverse energy jets are required to satisfy $E_T > 7.5$ and $6.5\,\mathrm{GeV}$, respectively. Both jets are required to lie in the pseudorapidity range $-1.5 < \eta < 2.0$. Differential cross sections have been measured and are confronted with the predictions from leading order Monte Carlo models and next-to-leading order QCD calculations.

1 Introduction

An important question which arises in hard diffractive processes is whether they can be factorized into universal diffractive parton distribution functions (PDFs) and the partonic cross section. At HERA, the diffractive PDFs have been extracted from QCD DGLAP fits to inclusive diffractive deep inelastic scattering (DIS) data [1, 2], where factorization is proven to hold [3, 4]. The factorization theorem and the universality of the extracted PDFs can be tested through exclusive processes with different hadronic final states. In particular, diffractive events with dijet production are important as they are sensitive to the diffractive gluon density (e.g. via $\gamma g \rightarrow q\bar{q}$ at HERA), which is known to carry most of the momentum of the diffractive exchange [1, 2, 5].

The H1 Collaboration has recently presented measurements of diffractive dijets in DIS [6] that support the factorization theorem. However, predictions of diffractive dijet cross sections at the Tevatron using the same PDFs overestimate the measurements by an order of magnitude [7]. The suppression of the Tevatron cross sections can be accounted for by considering rescattering processes between the two hadron beams which create additional particles that destroy the rapidity gap [8]. In one such model, a suppression factor of R=0.34 would also be expected to be observed in the resolved photoproduction of diffractive dijets at HERA [9]. Recent calculations at next-to-leading order (NLO) [10] agree with the diffractive dijet photoproduction measurements of the H1 Collaboration [11], if the resolved photon component is suppressed by R=0.34.

This paper presents measurements of the diffractive photoproduction of dijets made using the ZEUS detector at HERA. A 30-fold increase in luminosity has been achieved compared to the previous ZEUS analysis [12], which in combination with the addition of a new forward[1] detector, allows precise measurements to be made in a wider kinematic range. Measured differential cross sections are compared to leading order (LO) and NLO predictions which use the diffractive PDFs extracted from inclusive diffractive DIS measurements [1, 2].

2 Experimental set-up

This analysis uses an integrated luminosity of $77.6\,\text{pb}^{-1}$ collected with the ZEUS detector [13] at the HERA collider during the 1999 − 2000 data-taking period. The incoming

[1] The ZEUS coordinate system is a right-handed Cartesian system, with the Z axis pointing in the proton beam direction, referred to as the "forward direction", and the X axis pointing left towards the center of HERA. The coordinate origin is at the nominal interaction point.

positron[2] and proton energies were 27.5 and 920 GeV, respectively. The jets are reconstructed using the central tracking detector (CTD) [14] and uranium-scintillator calorimeter (CAL) [15]. Diffractive events are selected by requiring a large rapidity gap in the forward calorimeter (FCAL) and the forward plug calorimeter (FPC) [16], which was placed inside the FCAL, close to the beam pipe.

3 Kinematics and data selection

Diffractive dijet photoproduction processes ($ep \rightarrow ep + X(jet + jet + X')$) are characterized by a final state consisting of a scattered positron and a scattered proton, both of which escape down the beam pipe, and a hadronic system X, with invariant mass M_X, which contains the dijet system from the hard scattering. The kinematic variables describing this process are defined as follows:

- y, the fraction of the positron energy carried by the photon in the proton rest frame;
- Q^2, the photon virtuality;
- $x_{I\!P}$, the momentum fraction lost by the proton;
- $E_T^{jet1,2}$ and $\eta^{jet1,2}$, the transverse energy (E_T^{jet}) and pseudorapidity (η^{jet}) of the two highest E_T jets reconstructed by the k_T algorithm [17], which is run in the longitudinally invariant inclusive mode [18] in the laboratory frame.

The kinematic variables and jets are reconstructed from energy flow objects (EFOs) which combine energy clusters reconstructed in the CAL and charged tracks reconstructed in the CTD [19]. EFOs are additionally corrected for energy losses due to dead material in front of the CAL. The reconstructed values correspond well to their true values with good resolution, based on Monte Carlo studies. The jet energy resolution at an E_T around 7 GeV is approximately 15%.

The cross sections are measured in the following kinematic region:

- $0.2 < y < 0.85$, $Q^2 < 1.0\,\mathrm{GeV}^2$;
- $x_{I\!P} < 0.035$;
- $E_T^{jet1} > 7.5\,\mathrm{GeV}$, $E_T^{jet2} > 6.5\,\mathrm{GeV}$, $-1.5 < \eta^{jet1,2} < 2.0$.

Photoproduction events are selected by requiring that no scattered positron candidate is identified. Diffractive events are selected by requiring a large rapidity gap which covers the pseudorapidity range $3 < \eta < 5$, where $\eta \approx 5$ corresponds to the forward edge of the FPC. After applying these selection requirements, an additional 2% of the events

[2] Hereafter, "positron" is used to refer to both electron and positron beams.

are rejected as background from cosmic events based on the timing of the two highest E_T jets. Furthermore, the background from proton dissociation events, with a low-mass proton dissociative system escaping down the beam pipe, is estimated to be (16±4)% [20] and is subtracted from all measured cross sections. The contribution from non-diffractive background events is expected to be of the order of 10% and is not subtracted. A total of 10673 events remain after all selection cuts.

Two additional variables are used in this analysis:

$$z_{I\!P}^{obs} = \frac{\sum_{jets} E_T^{jet} e^{\eta^{jet}}}{2 x_{I\!P} E_p} \tag{1}$$

$$x_\gamma^{obs} = \frac{\sum_{jets} E_T^{jet} e^{-\eta^{jet}}}{2 y E_e} \tag{2}$$

where the sums run over the two highest E_T jets. The observable $z_{I\!P}^{obs}$ (x_γ^{obs}) is an estimator of the longitudinal fractional momentum taken from the diffractive exchange (photon) by the dijet system produced in the hard scattering. The observable $z_{I\!P}^{obs}$ is sensitive to the parton densities in the diffractive exchange, while the ranges x_γ^{obs} greater than 0.75 and less than 0.75 correspond to regions enriched with direct and resolved photon processes, respectively [21]. In direct photon processes, the entire photon participates in the hard scatter, whereas in resolved photon processes, the photon acts as a source of partons, with only a fraction of its momentum participating in the hard scatter.

4 Theoretical predictions

Data are compared to both LO and NLO predictions at the hadron level (i.e. level of stable hadrons).

The LO predictions are made using the RAPGAP Monte Carlo generator [22] interfaced to the parton shower model MEPS [23], and the hadronization model JETSET [24, 25]. The diffractive PDFs determined by the H1 Collaboration ("H1 fit 2") [1] and the photon structure function GRV-G-HO are used. This Monte Carlo generator is also used to correct the data to the hadron level.

Two sets of NLO QCD calculations are compared to the data: a model with resolved photon suppression by a factor of R=0.34 and a model with no suppression (R=1) [10]. The results of the recent preliminary QCD fits made by the H1 Collaboration ("H1 2002 fit (prel.)") are used for the diffractive parton densities [2]. In order to estimate the theoretical uncertainties, renormalization and factorization scales are varied from $0.5E_T^{jet1}$ to $2E_T^{jet1}$, where E_T^{jet1} is the E_T of the highest E_T jet. The parton level (i.e. level of partons after parton showers) predictions are corrected to the hadron level using correction factors determined with RAPGAP. Large hadronization corrections are observed at low $x_{I\!P}$ and high $z_{I\!P}^{obs}$. These corrections will be investigated further using a different hadronization model. The two highest x_γ^{obs} bins above 0.75 are combined to minimize the uncertainty of the correction factors in the two bins.

5 Results

The cross sections are measured as a function of y, $x_{I\!P}$, M_X, E_T^{jet1}, η^{jet1}, x_γ^{obs} and $z_{I\!P}^{obs}$. The largest systematic uncertainty comes from varying the size of the large rapidity gap requirement in data and RAPGAP. This is larger at higher $x_{I\!P}$: approximately 20% in the highest $x_{I\!P}$ bin.

The LO prediction from RAPGAP, normalized to the data by a factor of 0.52, gives a good description of the data, as seen in Figs. 1 and 2. In particular, the shape of the x_γ^{obs} distribution is well reproduced in both the direct and resolved enriched regions, as shown by the flat distribution of the ratio of data to RAPGAP. A lower ratio at lower x_γ^{obs} would indicate a suppression of resolved photon processes with respect to direct photon processes, when compared to RAPGAP.

The NLO QCD calculations after hadronization correction are also compared to the data in Figs. 3 and 4. The NLO predictions with resolved photon suppression (R=0.34) describe both the shape and normalization of the data fairly well. The predictions without resolved photon suppression (R=1) describe only the shape of the data. This could either indicate a suppression of resolved photon processes, or a global suppression (i.e. suppression of both direct and resolved photon processes). The x_γ^{obs} distribution is expected to be the most sensitive to any suppression of the resolved photon contribution. When the predictions are compared to the measured x_γ^{obs} distribution (Fig. 4), the description of the shape is better without any suppression, as demonstrated by the flatter distribution of the ratio of data to NLO. This could be an indication that a global suppression is more likely than a resolved photon suppression. However, there are other possible explanations, such as the uncertainty on the diffractive PDFs, in particular on the gluon density, to which this process is expected to be sensitive [2]. The impact of this uncertainty on the predictions is not currently known.

In summary, the predictions which do not consider a suppression of resolved photon processes with respect to direct photon processes give a reasonably good description of the shapes of the cross sections including x_γ^{obs}, at both LO and NLO. However at NLO, the normalization of the data is below predictions. Possible explanations include resolved photon suppression, the suppression of both direct and resolved photon processes, and the uncertainties arising from the diffractive PDFs.

References

[1] H1 Coll., C. Adloff et al., Z. Phys. **C 76**, 613 (1997).

[2] H1 Coll., *paper 980 submitted to 31. Intl. Conf. on High Energy Physics ICHEP 2002, Amsterdam, and paper 089 submitted to the EPS 2003 Conf., Aachen* (unpublished).

[3] J.C. Collins, Phys. Rev. **D57**, 3051 (1998).

[4] J.C. Collins, J. Phys. **G28**, 1069 (2002).

[5] ZEUS Coll., M. Derrick et al., Phys. Lett. **B 356**, 129 (1995).

[6] H1 Coll., C. Adloff et al., Eur. Phys. J. **C 20**, 29 (2001).

[7] CDF Coll., T. Affolder et al., Phys. Rev. Lett. **84**, 5043 (2000).

[8] A.B. Kaidalov, V.A. Khoze, A.D. Martin and M.G. Ryskin, Eur. Phys. J. **C21**, 521 (2001).

[9] A.B. Kaidalov, V.A. Khoze, A.D. Martin and M.G. Ryskin, Phys. Lett. **B567**, 61 (2003).

[10] M. Klasen and G. Kramer, Preprint DESY-04-011 (hep-ph/0401202), 2004.

[11] H1 Coll., *paper 987 submitted to 31. Intl. Conf. on High Energy Physics ICHEP 2002, Amsterdam, and paper 087 submitted to the EPS 2003 Conf., Aachen* (unpublished).

[12] ZEUS Coll., J. Breitweg et al., Eur. Phys. J. **C 5**, 41 (1998).

[13] ZEUS Coll., U. Holm (ed.), *The ZEUS Detector*. Status Report (unpublished), DESY (1993), available on `http://www-zeus.desy.de/bluebook/bluebook.html`.

[14] N. Harnew et al., Nucl. Inst. Meth. **A 279**, 290 (1989);
B. Foster et al., Nucl. Phys. Proc. Suppl. **B 32**, 181 (1993);
B. Foster et al., Nucl. Inst. Meth. **A 338**, 254 (1994).

[15] M. Derrick et al., Nucl. Inst. Meth. **A 309**, 77 (1991);
A. Andresen et al., Nucl. Inst. Meth. **A 309**, 101 (1991);
A. Caldwell et al., Nucl. Inst. Meth. **A 321**, 356 (1992);
A. Bernstein et al., Nucl. Inst. Meth. **A 336**, 23 (1993).

[16] ZEUS Coll., FPC group, A. Bamberger et al., Nucl. Inst. Meth. **A 450**, 235 (2000).

[17] S.Catani et al., Nucl. Phys. **B406**, 187 (1993).

[18] S.D. Ellis and D.E. Soper, Phys. Rev. **D 48**, 3160 (1993).

[19] G.M. Briskin, *Diffractive Dissociation in ep Deep Inelastic Scattering*. Ph.D. Thesis, Tel Aviv University, 1998. (Unpublished).

[20] ZEUS Coll., S. Chekanov et al., Nucl. Phys. **B672**, 3 (2003).

[21] ZEUS Coll., S. Chekanov et al., Eur. Phys. J. **C23**, 615 (2001).

[22] H. Jung, *The RAPGAP Monte Carlo for Deep Inelastic Scattering version 2.08/00* (unpublished). 2001.

[23] R.K. Ellis, W.J. Stirling and B.R. Webber, *QCD and Collider Physics*, Cambridge Monographs on Particle Physics, Nuclear Physics and Cosmology, Vol. 8. Cambridge University Press, 1996.

[24] M. Bengtsson and T. Sjöstrand, Comp. Phys. Comm. **46**, 43 (1987).

[25] T. Sjöstrand, Comp. Phys. Comm. **82**, 74 (1994).

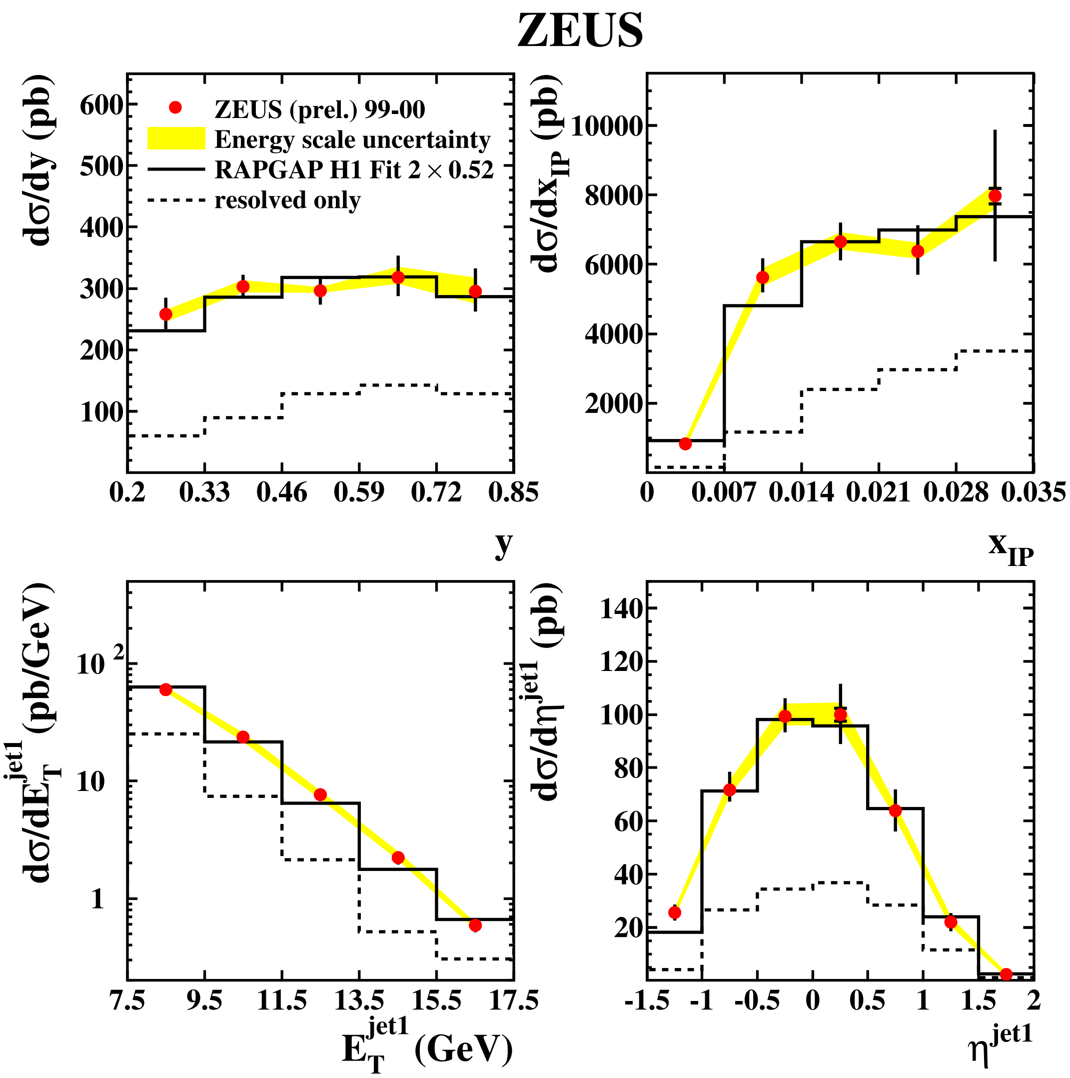

Figure 1: *The single differential cross sections in* y*,* $x_{I\!P}$*,* E_T^{jet1} *and* η^{jet1}*. The data are shown as dots, with the corresponding energy scale uncertainty shown as a band; the inner error bars indicate the statistical uncertainty and the outer error bars indicate the statistical and systematic uncertainties added in quadrature. The solid lines show the prediction of the LO RAPGAP Monte Carlo, normalized to the data by a factor of 0.52; the dashed lines are the resolved photon component from RAPGAP. The H1 Fit 2 diffractive PDFs are used [1].*

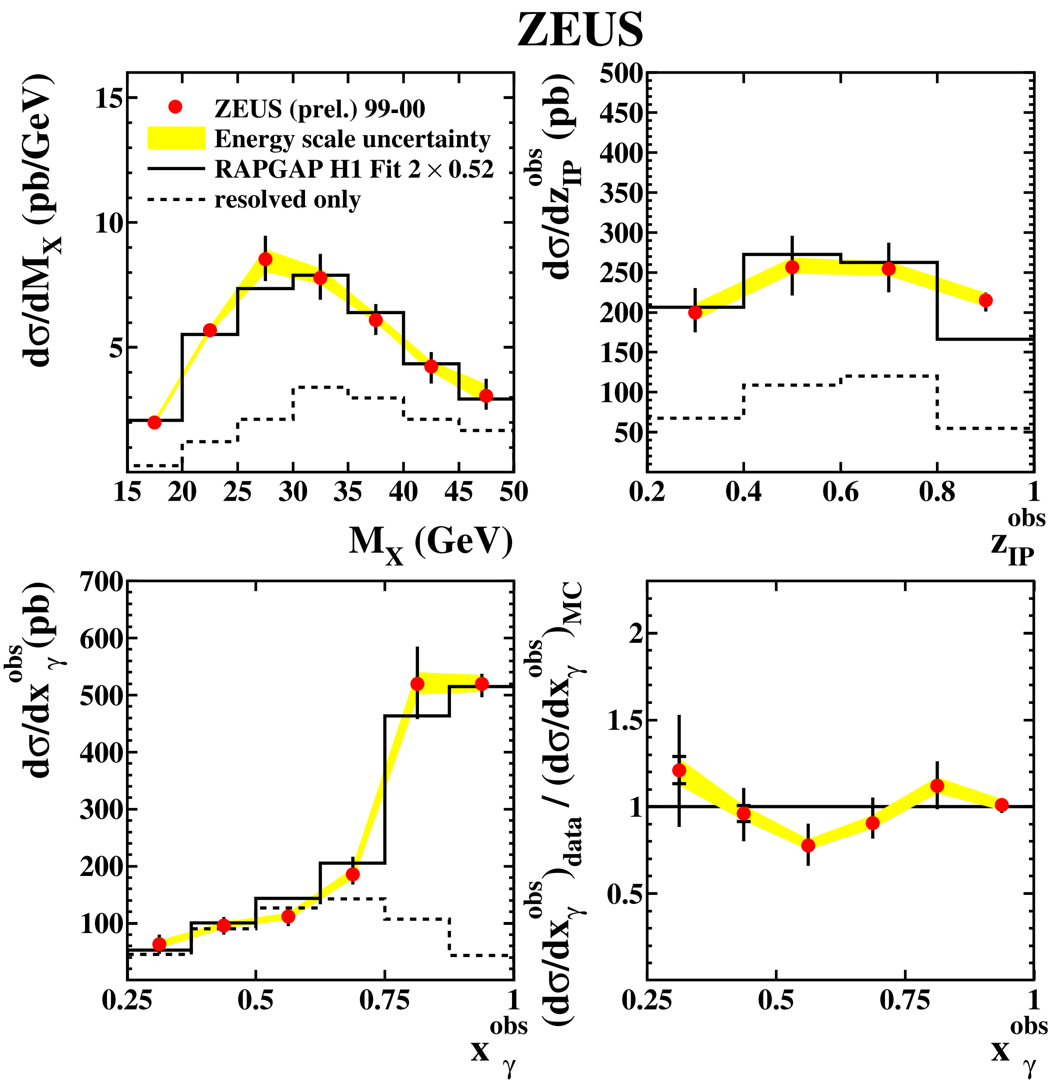

Figure 2: *The single differential cross sections in M_X, $z_{I\!P}^{obs}$, x_γ^{obs} and the ratio of the single differential cross section in x_γ^{obs} between data and RAPGAP normalized by 0.52. See the caption of Fig. 1 for a description of the data and the LO Monte Carlo prediction.*

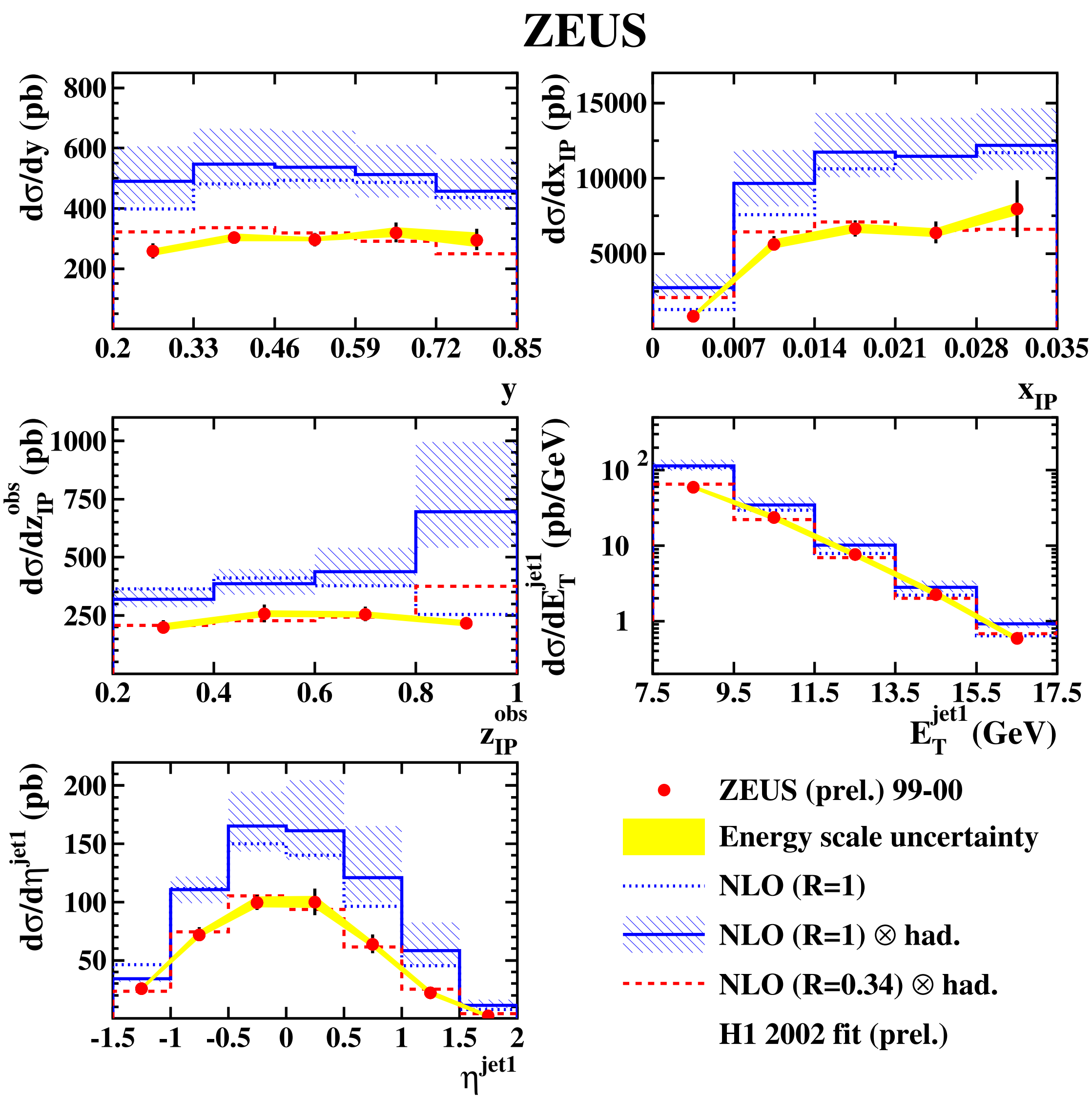

Figure 3: *The single differential cross sections in y, $x_{I\!P}$, $z_{I\!P}^{obs}$, E_T^{jet1} and η^{jet1}, compared to the NLO QCD predictions. For details of the data, see the caption of Fig. 1. The prediction without resolved photon suppression (R=1) and its theoretical uncertainty is shown as the solid lines with the shaded band; the corresponding parton level prediction before hadronization correction is shown as the dotted lines. The prediction with a suppression factor of 0.34 on the resolved photon processes (R=0.34) is shown as the dashed lines. The diffractive PDFs are from the H1 2002 fit [2].*

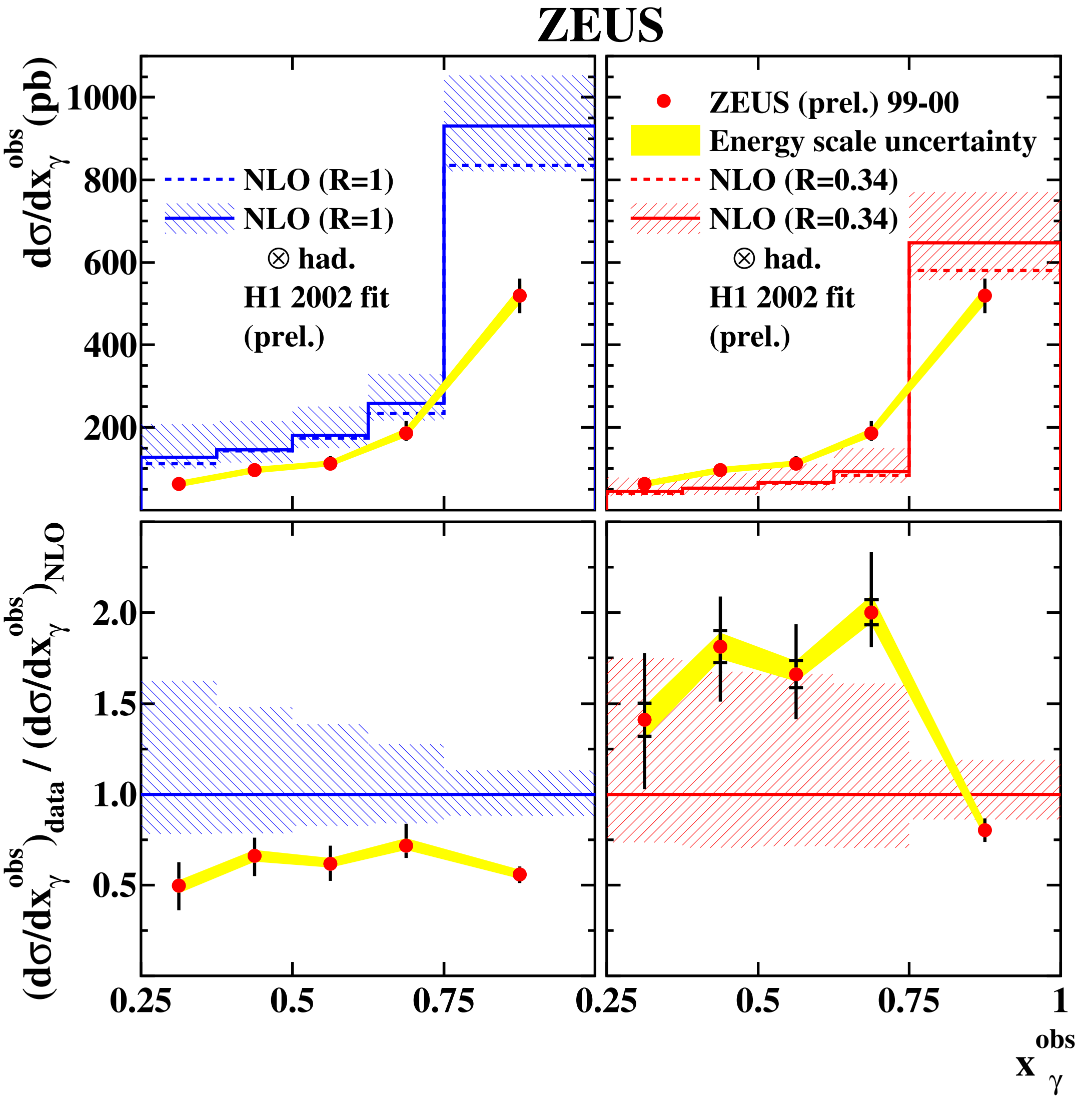

Figure 4: *The single differential cross section in x_γ^{obs} and the ratio of the single differential cross section in x_γ^{obs} between data and NLO, for the predictions without (R=1) and with (R=0.34) resolved photon suppression. See the caption of Fig. 1 for a description of the data. The solid lines with the shaded band indicate the predictions and their theoretical uncertainties; the dashed lines show the parton level predictions before hadronization correction. Refer to the caption of Fig. 3 for a description of the diffractive PDFs.*